Measurement of the three-body-recombination coefficient of ultracold lithium and strontium atoms

Bo-Yang Wang,[1,*] Yi-Fan Wang,[1,*] Zi-He An,[1] Li-Yang Xie,[1] Zhu-Xiong Ye,[1,†] Yi Zhang,[1] and Meng Khoon Tey[1,2,3,4,‡]

[1]*State Key Laboratory of Low-Dimensional Quantum Physics, Department of Physics, Tsinghua University, Beijing 100084, China*

[2]*Frontier Science Center for Quantum Information, Beijing, China*

[3]*Collaborative Innovation Center of Quantum Matter, Beijing, China*

[4]*Hefei National Laboratory, Hefei, Anhui 230088, China*

(Received 1 April 2024; accepted 8 July 2024; published 25 July 2024)

We report on the observation of a conspicuous loss in an ultracold mixture of ^{7}Li and ^{88}Sr atoms confined in a far-off-resonance optical dipole trap. We attribute the trap loss to the three-body inelastic Li-Sr-Sr collision and extract the corresponding three-body-recombination coefficient K_3 at $T \sim 18.5, 45, 70, 600$ μK. The measured three-body-recombination coefficient is about two to three orders of magnitude larger than the typical values convenient for realizing quantum degenerate gases, and essentially rules out the prospect of realizing ^{7}Li and ^{88}Sr mixtures of high phase space density. The measured three-body-recombination rates agree with the unitarity limit at high temperatures. Our results also confirm that the three-body-recombination loss is dominated by the light-heavy-heavy process, in agreement with the prediction for a system with a large mass-imbalanced and negligible intraspecies interaction.

DOI: 10.1103/PhysRevA.110.013322

I. INTRODUCTION

Ultracold mixtures of different atomic species provide unique opportunities to study exotic few-body and many-body physics such as Efimov states and strongly interacting quantum systems with mass-imbalanced components [1–5]. Ultracold molecules can facilitate precision measurements and tests of fundamental physical laws [6–8]. They also benefit the study of ultracold chemistry [9–11]. Among the possible platforms, dimers made up of alkali (AK) and alkaline-earth(-like) (AE) atoms have attracted much attention recently [12–20]. Compared to the more widely studied bialkalis, the AK-AE molecules possess both electric and magnetic dipole moments in their absolute ground state due to an unpaired electron. Besides allowing for more controls, the extra degree of freedom is expected to usher in much richer quantum phases and phenomena. They may be used for the studies of lattice-spin models [21], quantum magnetism [22], and exotic topological states of dipolar gas [23–26], etc.

When preparing an ultracold mixture of AK and AE atoms, the latter can usually be laser cooled directly to much lower temperatures using a narrow $^{1}S_0$-$^{3}P_1$ transition [27,28], and thus may be used to sympathetically cool its alkali partner [29–32]. Such a potential is, nevertheless, governed ultimately by the scattering properties between the two partners. To achieve effective sympathetic cooling [32–35], a rule of thumb is that the ratio of elastic to inelastic collisions should be larger than 100 [36,37]. The interspecies interactions also affect the stability and miscibility of the gases at high phase-space densities [38,39]. Therefore, understanding the scattering properties between the different components is the key to harvesting the advantages of these mixtures.

In our previous works [40,41], we found that ^{6}Li and various Sr isotopes have rather weak interspecies interactions. The magnitudes of their s-wave scattering lengths are of the order of 10 Bohr radii. In this paper, we investigate the stability of ^{7}Li and ^{88}Sr gas mixture in an far-off-resonant optical dipole trap. We find that a ^{7}Li and ^{88}Sr mixture exhibits a severe Li-Sr-Sr three-body collision loss at ultracold temperatures, regardless of the magnetic field strengths. By measuring the relevant three-body-recombination coefficients K_3 at various temperatures, we conclude that the measured K_3 coefficients at ultracold temperatures are about two to three orders of magnitude larger than the typical values convenient for realizing quantum degenerate gases.

II. EXPERIMENTAL PROCEDURES

The optical layout around our science chamber is illustrated in Fig. 1. Its details have been described in our previous works [40,41]. To give some useful numbers, the pressure of our science chamber is about 5×10^{-11} Torr. The Sr atom number at the beginning of this three-body loss measurement ranges from 5×10^{6} to 2×10^{7}, while the Li atom number ranges from 1.5×10^{5} to 3.5×10^{5}. Taking the temperatures of the gas into account, the corresponding number densities at the center of the optical dipole trap are $(8–30) \times 10^{13}$

*These authors contributed equally to this work.

†Present address: State Key Laboratory of Quantum Optics and Quantum Optics Devices, Institute of Opto-Electronics, Shanxi University, Taiyuan, Shanxi 030006, China.

‡Contact author: mengkhoon_tey@mail.tsinghua.edu.cn

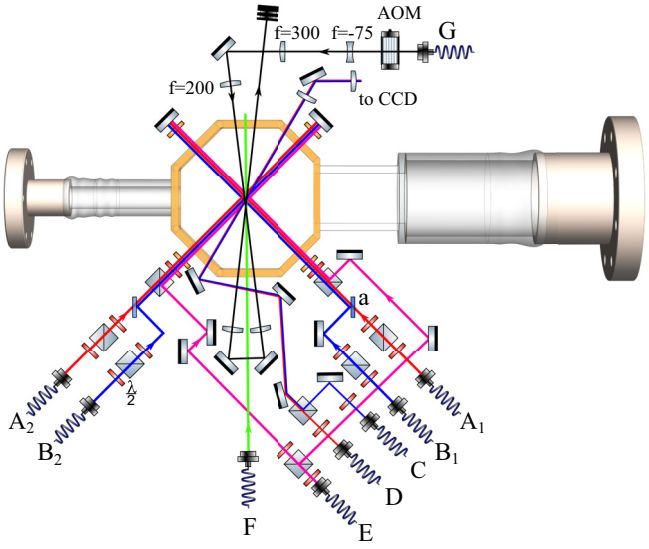

FIG. 1. Optical layout around the science chamber. Zeeman slowed atomic beams enter the chamber from the left through a common dual-species Zeeman slower. $A_{1,2}$ guides the 671- and 689-nm light for performing Li and Sr red MOTs, respectively. $B_{1,2}$: 461-nm light for Sr blue MOT. C: Sr imaging beam. D: Li imaging beam. E: gray molasses beams for Li. F: Sr repumping light (679 and 707 nm). G: 1064-nm crossed optical dipole trap (CODT). a: dichroic beam splitter.

cm^{-3} for ^{88}Sr, and (2–5) $\times$ 10^{12} cm^{-3} for ^{7}Li. The reported three-body-recombination results are obtained at zero magnetic field.

We measure the interspecies collision loss rate using the following experimental procedures. We begin by cooling and trapping Sr atoms in a blue magneto-optical (MOT) trap using the broad 461-nm $^1S_0 \rightarrow {}^1P_1$ transition (linewidth 30.5 MHz). Upon completion of the blue-MOT loading, the ~2 mK atoms are further cooled in a red MOT to 5 μK using the narrow $^1S_0 \rightarrow {}^3P_1$ intercombination transition at 689 nm (linewidth 7.5 kHz). During the red-MOT stage, the power of a far-off-resonant crossed optical-dipole trap (CODT) is ramped to 14 W to store the Sr atoms. The CODT is formed by intersecting two 1064-nm light beams, both with a waist 30 μm, at 10°.

After trapping Sr atoms, Li atoms are magneto-optically trapped using the 671-nm D_2 transition. To reduce the loss of Sr atoms due to the light-assisted collision with the Li atoms, we move the Li MOT away from the Sr atoms in the CODT by changing the current of the third-stage Zeeman slower coil. Upon completion of the Li atoms loading, we compress the Li cloud by increasing the magnetic field gradient and, at the same time, move the Li atoms to overlap with the CODT. Finally, we cool the Li atoms to about 20 μK and transfer them into the CODT through an 11-ms-long gray-molasses (GM) [42] cooling process. The ^{7}Li atoms are pumped to the $F = 1$ hyperfine ground state in the end, resulting in a mixture containing all three Zeeman sublevels.

The trap-depth ratio for Li and Sr is $U_{\rm Li}/U_{\rm Sr} = 1.1$ for a 1064-nm trap. As it is much easier to obtain a larger and colder sample of Sr, the Sr sympathetically cools the Li to a common temperature that depends on the final trap depth of the CODT. To study the interaction properties, we hold the mixture in the CODT for a variable time and perform time-of-flight absorption imaging after switching off the CODT to determine the atom number and the temperature of each species. The overall experimental sequence is detailed in Fig. 2.

III. RESULTS

Figure 3(a) shows the typical loss curves of ^{7}Li atoms mixed with various numbers of ^{88}Sr atoms at a temperature of $T \sim 600$ μK. Here, the time $t = 0$, and in all other measurements, is chosen to be the instance when the two species become thermalized at the desired temperatures. For $T_{\rm Li} = T_{\rm Sr} \sim 600$ μK, this instance is 50 ms after both atoms are loaded into CODT. In the absence of Sr atoms, the trapped ^{7}Li atoms exhibit a $1/e$ lifetime of 9.1 s, limited by collision with the background gases and plain evaporation, giving a $K_1 \approx 0.11$ s^{-1}. The presence of Sr atoms results in a heavy loss of ^{7}Li atoms. By plotting the ^{7}Li number in logarithmic scales, it is clear that all the decay curves can be very well fitted with a single-exponent $\propto \exp(-t/\tau)$, resulting in $1/e$ lifetimes τ between 40 and 200 ms.

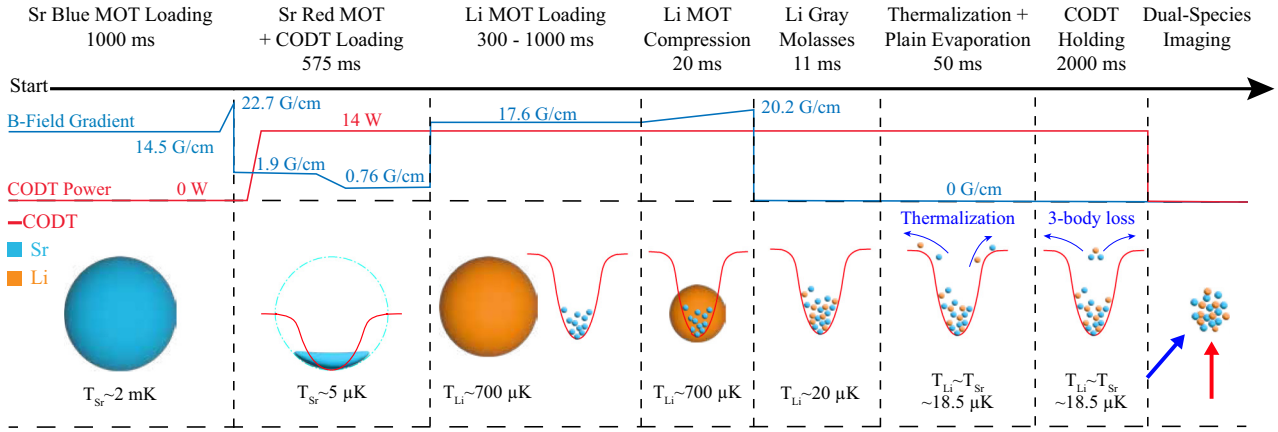

FIG. 2. A typical experimental sequence. The power of the dipole trap is varied to perform measurements at different temperatures. The Li MOT loading time is varied to control the relative abundance between Li and Sr atoms.

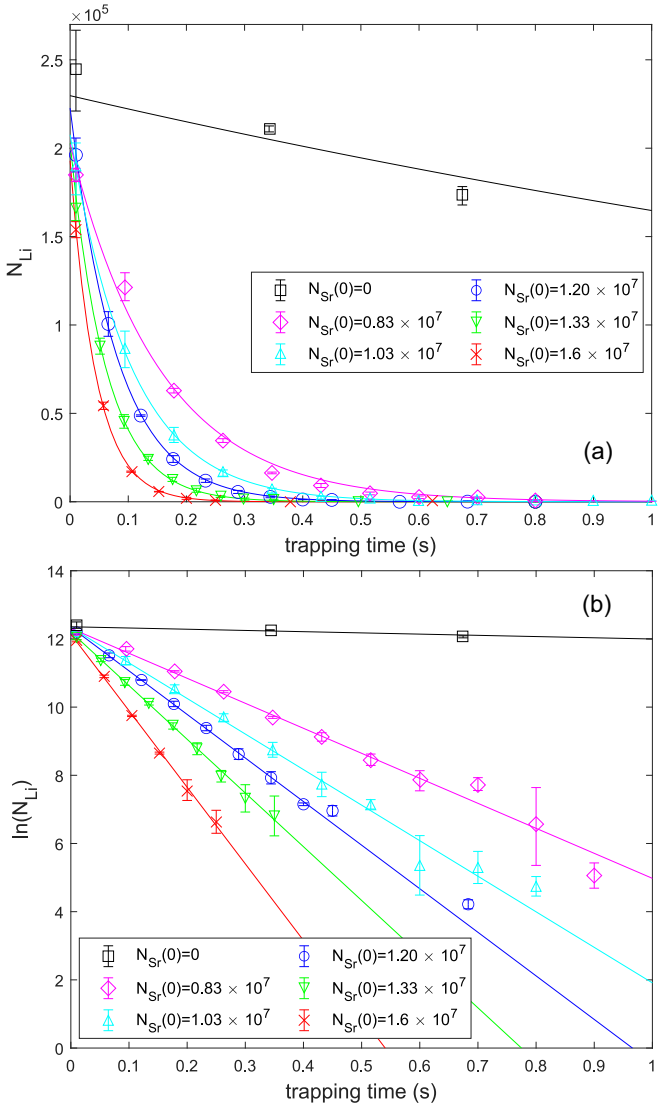

FIG. 3. (a) Decay of atom numbers of ^{7}Li in the $F = 1$ hyperfine ground state in the CODT over trapping time vs a set of ^{88}Sr atom numbers. Some error bars are smaller than the symbol size. The data are fitted with exponential functions (solid lines). (b) Same data as in (a) but using a logarithmic scale in the y axis. The solid straight lines are linear fits which highlight the single-exponent nature of these decays.

We find that the enhanced atom losses are mainly caused by the three-body recombination of Li-Sr-Sr. This conclusion is reached by considering the following loss mechanisms and observations. We first consider atom loss due to evaporative cooling. The loss rate of evaporative cooling is proportional to $\eta_i e^{-\eta_i}$ [43], where $\eta_i = U_i/k_B T_i$ is the parameter defining the trap depth relative to the thermal energy of an atom. As we set the starting time $t = 0$ such that $\eta_{\rm Li} \sim \eta_{\rm Sr} \sim 10$, the single-particle atom loss caused by plain evaporation can be neglected within tens of ms. To exclude intraspecies inelastic collision loss, we measure the single-species lifetime of Li and Sr in the CODT in the absence of another species. We find that their respective lifetimes are independent of the gas density within our parameter range, indicating a negligible intraspecies collision loss. These results are to be expected due to the small s-wave scattering lengths for two $F = 1$ ^{7}Li atoms (less than $18.2a_0$ for any m_F combinations; see Table I of Ref. [44]) and for two ^{88}Sr atoms in the ground state ($a \sim -1.4a_0$ [45]) at zero magnetic field.

With regard to the interspecies collision loss, the Li-Sr two-body inelastic collision is essentially forbidden due to the lack of a magnetic dipole moment in the $^1S_0$ ground state of ^{88}Sr. In contrast, a magnetic dipole-dipole interaction is responsible for two-body dipolar spin-exchange relaxation in the bialkali system. As for interspecies three-body recombination, two processes may occur—the light-heavy-heavy recombination Li-Sr-Sr and the light-light-heavy recombination Li-Li-Sr. When we load much more Li than Sr ($N_{\rm Li} \sim 2 \times 10^6$, $N_{\rm Sr} \sim 5 \times 10^4$) and measure the loss rate of Sr, we do not observe enhanced Sr loss proportional to $N_{\rm Li}^2$. However, a remarkable loss of ^{7}Li is observed when we load more Sr than Li ($N_{\rm Li} \sim 5 \times 10^4$, $N_{\rm Sr} \sim 2 \times 10^6$). The above measurements thereby rule out Sr-Li-Li three-body loss as being a major source for the measurement results presented in Fig. 3 and the atom loss we observe should be attributed predominantly to the Li-Sr-Sr process. This observation of a dominating light-heavy-heavy process is in agreement with a number of experimental observations and theoretical predictions [46–49].

In order to measure the three-body loss coefficient of Li-Sr-Sr, we make Sr two orders of magnitude more abundant than Li to enhance the Li-Sr-Sr process, and perform a series of experiments with different $N_{\rm Sr}$ and extract the Li-Sr-Sr three-body loss coefficient by fitting the Li loss rate versus $N_{\rm Sr}^2$. For the mixture conditions we consider, the measured loss rate of the ^{7}Li atoms in the Li-Sr mixtures can be described by

$$\frac{dN_{\rm Li}}{dt} = -K_1 N_{\rm Li} - K_3 \int n_{\rm Li}(\vec{r}) n_{\rm Sr}^2(\vec{r}) d^3\vec{r}, \qquad (1)$$

where $n(\vec{r})$ represents the atom number density at position $\vec{r}$. Here, the coefficient for the single-particle loss, K_1, is mainly determined by the amount of background gases in the vacuum chamber, whereas the coefficient for the Li-Sr-Sr three-body-recombination rate, K_3, depends intrinsically on the temperature, the statistical nature, and the interatomic potentials of the relevant atoms.

The fact that the ^{7}Li decay curves are well represented by simple exponential functions is puzzling, given that the second term in Eq. (1) depends on the local densities $n_{\rm Li}(\vec{r})$ instead of the total atom number $N_{\rm Li}$. It turns out that this phenomenon can be explained by the fast diffusion and rethermalization of the Li and Sr atoms in the trap (relative to the measured decay lifetimes τ). The former is guaranteed by the high trapping frequencies and the latter can be attributed to efficient two-body scattering, a feature which usually comes hand in hand with fast three-body loss. As evidence, we present in Fig. 4 the measured linear probability distributions of ^{7}Li atoms along the long axis of the CODT after certain trapping times. It is clear that the probability distributions of the ^{7}Li atoms remain unchanged despite a large drop in the remaining atom number from 1.6×10^5 ($t = 64$ ms) to 3.0×10^4 ($t = 224$ ms), and can be well fitted by a Boltzmann distribution $f_{\rm B}(\vec{r}) \propto e^{-U(\vec{r})/k_{\rm B}T}$, where $U(\vec{r})$ represents the trap potential. The same phenomenon is observed for the Sr.

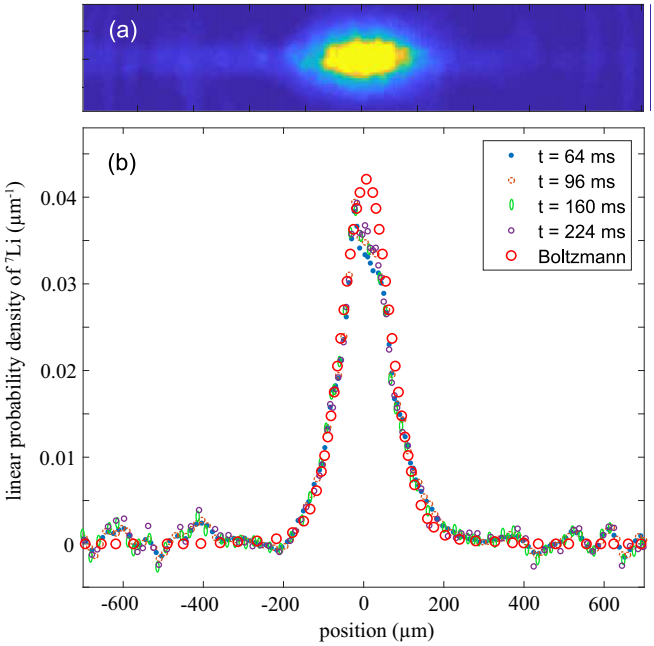

FIG. 4. (a) An example of an *in situ* image of ^{7}Li atoms in the CODT. (b) Probability distributions of ^{7}Li atoms along the long axis of the CODT after various trapping times ($t = 64, 96, 160, 224$ ms) (solid dots), obtained by dividing the measured linear density by the total atom number. Despite the atom loss over time, the probability distributions remain unchanged and their wings can be well fitted by a theoretical distribution of a thermal gas at 600 μK (red line). The deviation near the cloud center is caused by the nonlinear absorption effects due to large atom densities of the order of 5×10^{12} cm^{-3}.

Because of the fast thermalization behavior, we can rewrite Eq. (1) by replacing the local atom density $n_{\mathrm{Li(Sr)}}(\vec{r})$ by $N_{\mathrm{Li(Sr)}} f_{\mathrm{B,Li(Sr)}}(\vec{r}, T)$, where f_{B} represents the Boltzmann probability density distribution, giving

$$\frac{dN_{\mathrm{Li}}}{dt} = -K_1 N_{\mathrm{Li}} - K_3 N_{\mathrm{Li}} N_{\mathrm{Sr}}^2 \mathcal{D}_{\mathrm{LiSrSr}}, \tag{2}$$

where $\mathcal{D}_{\mathrm{LiSrSr}} = \int_0^\infty f_{\mathrm{B,Li}}(\vec{r}, T) f_{\mathrm{B,Sr}}^2(\vec{r}, T) d^3\vec{r}$ can be calculated from the properties of the CODT as well as the temperature of the mixtures. As the measured change in the Sr atom number N_{Sr} is less than 5% in 1 s, if we neglect the small decrease in N_{Sr}, we can obtain from Eq. (2) an approximate ^{7}Li decay rate of

$$1/\tau = K_1 + K_3 N_{\mathrm{Sr}}^2 \mathcal{D}_{\mathrm{LiSrSr}}. \tag{3}$$

This formula explains why the decay of Li atoms takes a simple exponential form in Fig. 3.

In Fig. 5, we plot the loss rate $1/\tau$ extracted from Fig. 3(b) as a function of $N_{\mathrm{Sr}}^2 \mathcal{D}_{\mathrm{LiSrSr}}$. The resulting data fall well on a straight line in agreement with Eq. (3). The slope of the least-squares linear fit gives a three-body-recombination coefficient $K_3 = (4.8 \pm 0.7) \times 10^{-28}$ cm^6/s. This result is, nevertheless, an underestimation since we ignore the slight decay in N_{Sr}. Taking into account the loss in Sr and fitting the measurement results in Fig. 3 using Eq. (2) directly gives $K_3 = (5.7 \pm 1.6) \times 10^{-28}$ cm^6/s. The reported uncertainty here and those after include estimated systematic errors.

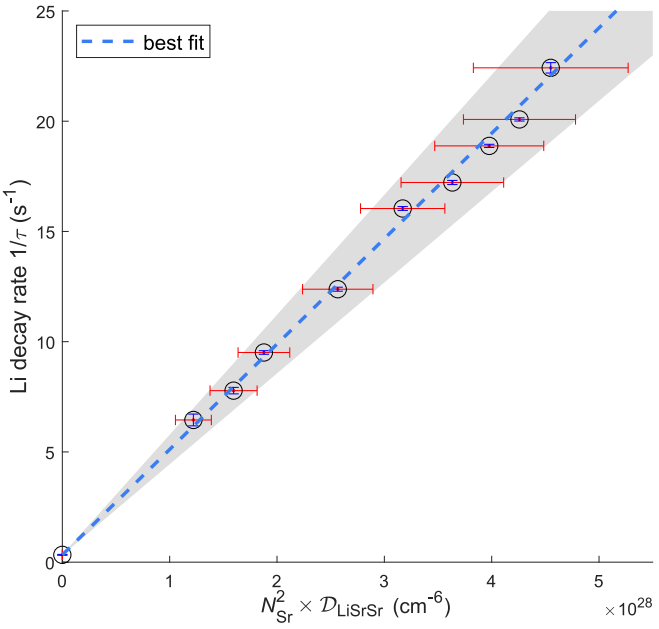

FIG. 5. A least-squares linear fitting of ^{7}Li decay rate $1/\tau$ vs $N_{\mathrm{Sr}}^2 \times \mathcal{D}_{\mathrm{LiSrSr}}$. The dashed blue line is the best fit and the fitting error is represented by the gray shaded area. Some statistical error bars are smaller than the symbol size.

By repeating the above-mentioned procedures for $T = 18.5, 45, 70$ μK, we obtain K_3 at each temperature as displayed in Table I. The measured K_3 becomes larger as the gas temperature drops and saturates to a constant within measurement uncertainty at temperatures below 70 μK. Unfortunately, due to the heavy atom loss during evaporative cooling, we are unable to perform measurements at even lower temperatures. Compared to ^{87}Rb whose three-body-recombination coefficient is $(4.3 \pm 1.8) \times 10^{-29}$ cm^6 s^{-1} at $T = 800$ nK [50], the K_3 of Li-Sr-Sr is about three orders of magnitude larger at ultracold temperatures.

IV. ANALYSIS ON THE OBSERVED THREE-BODY RECOMBINATION

Enhanced three-body loss can be caused by a diverging two-body scattering length or an incidental three-body resonance. However, the latter, which represents a resonance in a true three-body potential when the two-body scattering length is small, has not been identified in previous experiments. We therefore believe the strong three-body loss observed in our work is most likely a result of the former. Furthermore, because the temperatures studied in this work are much lower than the height of the Li-Sr p-wave barrier, which is about k_B

TABLE I. Measured K_3 at various temperatures.

T (μK)	K_3 (cm^6 s^{-1})
18.5	$(1.3 \pm 0.5) \times 10^{-26}$
46	$(1.4 \pm 0.5) \times 10^{-26}$
70	$(1.5 \pm 0.5) \times 10^{-26}$
600	$(5.7 \pm 1.6) \times 10^{-28}$

(2.08 mK), the enhanced loss observed across a wide range of temperatures should be attributed to a large *s*-wave scattering length, even though a *p*-wave shape resonance cannot be excluded completely. This hypothesis is consistent with the mass-scaling prediction [51] derived from the latest Li-Sr potential [52], aided with the *s*-wave scattering lengths of ^{6}Li - ^{88}Sr and ^{6}Li - ^{84}Sr as measured via interspecies thermalization [40,41].

Notably, the large ^{7}Li - ^{88}Sr *s*-wave scattering length is not caused by a Feshbach resonance. This assertion is confirmed by our observation that the atom loss rates are not affected by magnetic field strengths. This fact is not surprising since ^{88}Sr in its ground state has neither electronic spin nor nuclear spin. Therefore, the molecular potential of the ^{7}Li - ^{88}Sr molecule is essentially a single-channel potential in the electronic ground state, which does not support any strong Feshbach resonance [19].

In Ref. [48], Petrov and Werner considered the three-body recombination in heteronuclear mixtures at finite temperatures. Incidentally, our scenario coincides with case (i) in their study, where the light-heavy particles feature a large scattering length and there is essentially no interaction between the heavy-heavy particles. They demonstrated that when the temperature is sufficiently high such that the thermal de Broglie wavelength $\lambda = \hbar\sqrt{2\pi/\mu k_B T}$ is smaller than the scattering length a, the three-body-recombination coefficient is bounded above by [48]

$$K_{\max} = \frac{32\pi^2\hbar^5\cos^3\phi}{m^3(k_B T)^2}. \tag{4}$$

Here, the generalized reduced mass is $m = 2(m_{\rm Li}m_{\rm Sr})/(m_{\rm Li} + m_{\rm Sr})$ and ϕ is defined by $\sin\phi = m_{\rm Sr}/(m_{\rm Li} + m_{\rm Sr})$. Consequently, $K_{\max}$ is approximately 4×10^{-25}, 7×10^{-26}, 3×10^{-26}, and 4×10^{-28} cm^6 s^{-1} for $T = 18.5, 46, 70,$ and 600 μK, respectively. It is remarkable that the measured value at 600 μK coincides with the $K_{\max}$ within measurement uncertainty. At 70 μK, the measured value is close to, but about half of, $K_{\max}$. At even lower temperatures, the measured K_3 becomes a constant within measurement uncertainties and is much smaller than $K_{\max}$. As the saturation behavior is expected to occur when a becomes smaller than $\lambda_{\rm th}$ (see Fig. 2 of Ref. [48] for an illustration), our results provide an upper bound to the *s*-wave scattering length of ^{7}Li and ^{88}Sr atoms. Since the onset of saturation occurs around 70 μK, we infer that the magnitude of the ^{7}Li - ^{88}Sr scattering length is likely on the order of several hundred a_0 [48,53]. A conclusive determination of the *s*-wave scattering length, however, requires spectroscopic measurement of the weakly bound ^{7}Li - ^{88}Sr molecules.

V. CONCLUSION

In summary, we investigate the three-body-recombination loss in a bosonic mixture of ^{7}Li and ^{88}Sr. Significant losses are observed at $T = 18.5, 45, 70, 600$ μK in a crossed optical dipole trap and the corresponding three-body-recombination coefficients of Li-Sr-Sr process are determined. Our results confirm that the three-body-recombination loss is predominantly driven by the light-heavy-heavy process, as expected for a system with large mass imbalance and negligible intraspecies interaction [46,48,49]. Our observation essentially rules out the feasibility of realizing large sample of a doubly degenerate mixture of ^{7}Li and ^{88}Sr atoms. Moreover, our results imply that the magnitude of the ^{7}Li - ^{88}Sr *s*-wave scattering length is of the order of several hundred Bohr radii.

ACKNOWLEDGMENTS

We thank Gao-Ren Wang, Michał Tomza, Peng Zhang, Xiao-Ling Cui, and Zhen-Hua Yu for fruitful discussions. M.K.T. thanks an anonymous referee for his/her constructive criticisms and illuminating suggestions. We gratefully acknowledge the support by the National Natural Science Foundation of China (NSFC) (Grant No. 12234012), and the National Key R&D Program of China (Grant No. 2018YFA0306503).

[1] C. Kohstall, M. Zaccanti, M. Jag, A. Trenkwalder, P. Massignan, G. M. Bruun, F. Schreck, and R. Grimm, Nature (London) **485**, 615 (2012).
[2] R. Pires, J. Ulmanis, S. Häfner, M. Repp, A. Arias, E. D. Kuhnle, and M. Weidemüller, Phys. Rev. Lett. **112**, 250404 (2014).
[3] R. A. W. Maier, M. Eisele, E. Tiemann, and C. Zimmermann, Phys. Rev. Lett. **115**, 043201 (2015).
[4] R. S. Bloom, M.-G. Hu, T. D. Cumby, and D. S. Jin, Phys. Rev. Lett. **111**, 105301 (2013).
[5] S.-K. Tung, K. Jimenez-Garcia, J. Johansen, C. V. Parker, and C. Chin, Phys. Rev. Lett. **113**, 240402 (2014).
[6] T. Zelevinsky, S. Kotochigova, and J. Ye, Phys. Rev. Lett. **100**, 043201 (2008).
[7] J. J. Hudson, D. M. Kara, I. Smallman, B. E. Sauer, M. R. Tarbutt, and E. A. Hinds, Nature (London) **473**, 493 (2011).
[8] L. D. Carr, D. DeMille, R. V. Krems, and J. Ye, New J. Phys. **11**, 055049 (2009).
[9] S. Ospelkaus, K.-K. Ni, D. Wang, M. De Miranda, B. Neyenhuis, . G. Quéméner, P. Julienne, J. Bohn, D. Jin, and J. Ye, Science **327**, 853 (2010).
[10] R. V. Krems, Phys. Chem. Chem. Phys. **10**, 4079 (2008).
[11] H. Yang, X.-Y. Wang, Z. Su, J. Cao, D.-C. Zhang, J. Rui, B. Zhao, C.-L. Bai, and J.-W. Pan, Nature (London) **602**, 229 (2022).
[12] T. Franzen, B. Pollklesener, C. Sillus, and A. Görlitz, Phys. Rev. A **107**, 023114 (2023).
[13] B. Mukherjee, M. D. Frye, and J. M. Hutson, Phys. Rev. A **105**, 023306 (2022).
[14] A. Ciamei, J. Szczepkowski, A. Bayerle, V. Barbé, L. Reichsöllner, S. M. Tzanova, C.-C. Chen, B. Pasquiou, A. Grochola, P. Kowalczyk, W. Jastrzebski, and F. Schreck, Phys. Chem. Chem. Phys. **20**, 26221 (2018).
[15] A. Green, H. Li, J. H. See Toh, X. Tang, K. C. McCormick, M. Li, E. Tiesinga, S. Kotochigova, and S. Gupta, Phys. Rev. X **10**, 031037 (2020).

[16] D. A. Brue and J. M. Hutson, Phys. Rev. Lett. **108**, 043201 (2012).
[17] T. Franzen, A. Guttridge, K. E. Wilson, J. Segal, M. D. Frye, J. M. Hutson, and S. L. Cornish, Phys. Rev. Res. **4**, 043072 (2022).
[18] F. Schäfer, H. Konishi, A. Bouscal, T. Yagami, M. D. Frye, J. M. Hutson, and Y. Takahashi, J. Phys.: Conf. Ser. **1412**, 062005 (2020).
[19] V. Barbé, A. Ciamei, B. Pasquiou, L. Reichsöllner, F. Schreck, P. S. Żuchowski, and J. M. Hutson, Nat. Phys. **14**, 881 (2018).
[20] A. Guttridge, M. D. Frye, B. C. Yang, J. M. Hutson, and S. L. Cornish, Phys. Rev. A **98**, 022707 (2018).
[21] A. Micheli, G. Brennen, and P. Zoller, Nat. Phys. **2**, 341 (2006).
[22] A. V. Gorshkov, S. R. Manmana, G. Chen, J. Ye, E. Demler, M. D. Lukin, and A. M. Rey, Phys. Rev. Lett. **107**, 115301 (2011).
[23] D. Peter, S. Müller, S. Wessel, and H. P. Büchler, Phys. Rev. Lett. **109**, 025303 (2012).
[24] N. R. Cooper and G. V. Shlyapnikov, Phys. Rev. Lett. **103**, 155302 (2009).
[25] B. M. Fregoso and E. Fradkin, Phys. Rev. Lett. **103**, 205301 (2009).
[26] N. Y. Yao, M. P. Zaletel, D. M. Stamper-Kurn, and A. Vishwanath, Nat. Phys. **14**, 405 (2018).
[27] H. Katori, T. Ido, Y. Isoya, and M. Kuwata-Gonokami, Phys. Rev. Lett. **82**, 1116 (1999).
[28] T. Binnewies, G. Wilpers, U. Sterr, F. Riehle, J. Helmcke, T. E. Mehlstäubler, E. M. Rasel, and W. Ertmer, Phys. Rev. Lett. **87**, 123002 (2001).
[29] H. Hara, Y. Takasu, Y. Yamaoka, J. M. Doyle, and Y. Takahashi, Phys. Rev. Lett. **106**, 205304 (2011).
[30] V. V. Ivanov, A. Khramov, A. H. Hansen, W. H. Dowd, F. Münchow, A. O. Jamison, and S. Gupta, Phys. Rev. Lett. **106**, 153201 (2011).
[31] K. E. Wilson, A. Guttridge, J. Segal, and S. L. Cornish, Phys. Rev. A **103**, 033306 (2021).
[32] B. Pasquiou, A. Bayerle, S. M. Tzanova, S. Stellmer, J. Szczepkowski, M. Parigger, R. Grimm, and F. Schreck, Phys. Rev. A **88**, 023601 (2013).
[33] G. Modugno, G. Ferrari, G. Roati, R. J. Brecha, A. Simoni, and M. Inguscio, Science **294**, 1320 (2001).
[34] M. Mudrich, S. Kraft, K. Singer, R. Grimm, A. Mosk, and M. Weidemüller, Phys. Rev. Lett. **88**, 253001 (2002).
[35] M. Anderlini, E. Courtade, M. Cristiani, D. Cossart, D. Ciampini, C. Sias, O. Morsch, and E. Arimondo, Phys. Rev. A **71**, 061401(R) (2005).
[36] J. P. Burke, Jr. J. L. Bohn, B. D. Esry, and C. H. Greene, Phys. Rev. Lett. **80**, 2097 (1998).
[37] R. deCarvalho, J. M. Doyle, B. Friedrich, T. Guillet, J. Kim, D. Patterson, and J. D. Weinstein, Eur. Phys. J. D **7**, 289 (1999).
[38] S. L. Cornish, N. R. Claussen, J. L. Roberts, E. A. Cornell, and C. E. Wieman, Phys. Rev. Lett. **85**, 1795 (2000).
[39] S. B. Papp, J. M. Pino, and C. E. Wieman, Phys. Rev. Lett. **101**, 040402 (2008).
[40] X.-B. Ma, Z.-X. Ye, L.-Y. Xie, Z. Guo, L. You, and M. K. Tey, Chin. Phys. Lett. **36**, 073401 (2019); Erratum: **36**, 109902 (2019).
[41] Z.-X. Ye, L.-Y. Xie, Z. Guo, X.-B. Ma, G.-R. Wang, L. You, and M. K. Tey, Phys. Rev. A **102**, 033307 (2020).
[42] A. T. Grier, I. Ferrier-Barbut, B. S. Rem, M. Delehaye, L. Khaykovich, F. Chevy, and C. Salomon, Phys. Rev. A **87**, 063411 (2013).
[43] O. J. Luiten, M. W. Reynolds, and J. T. M. Walraven, Phys. Rev. A **53**, 381 (1996).
[44] S. J. Huh, K. Kim, K. Kwon, and J.-Y. Choi, Phys. Rev. Res. **2**, 033471 (2020).
[45] Y. N. Martinez de Escobar, P. G. Mickelson, P. Pellegrini, S. B. Nagel, A. Traverso, M. Yan, R. Côté, and T. C. Killian, Phys. Rev. A **78**, 062708 (2008).
[46] M. Mikkelsen, A. S. Jensen, D. V. Fedorov, and N. T. Zinner, J. Phys. B: At., Mol. Opt. Phys. **48**, 085301 (2015).
[47] Z.-X. Ye, A. Canali, E. Soave, M. Kreyer, Y. Yudkin, C. Ravensbergen, E. Kirilov, and R. Grimm, Phys. Rev. A **106**, 043314 (2022).
[48] D. S. Petrov and F. Werner, Phys. Rev. A **92**, 022704 (2015).
[49] E. Braaten and H.-W. Hammer, Phys. Rep. **428**, 259 (2006).
[50] E. A. Burt, R. W. Ghrist, C. J. Myatt, M. J. Holland, E. A. Cornell, and C. E. Wieman, Phys. Rev. Lett. **79**, 337 (1997).
[51] M. Tomza (private communication).
[52] H. Ladjimi and M. Tomza, Phys. Rev. A **109**, 052814 (2024).
[53] B. S. Rem, A. T. Grier, I. Ferrier-Barbut, U. Eismann, T. Langen, N. Navon, L. Khaykovich, F. Werner, D. S. Petrov, F. Chevy, and C. Salomon, Phys. Rev. Lett. **110**, 163202 (2013).